

Research Article

Application of acidic treated peanut shell biochar in methyl orange removal from aqueous medium: Elucidating isotherms, kinetics and proposed mechanism



Check for updates

Erik S. Pereira , Ralf R. R. Junior* , Sandro J. Andrade

ABSTRACT: The urgent need for sustainable water treatment solutions has driven global scientific efforts toward developing novel materials. Biochar, a low-cost material produced from biomass waste, represents a promising and versatile adsorbent class. In this study, acid-treated peanut shell biochar (PS-BC) was synthesized and evaluated for the removal of the methyl orange (MO) dye from aqueous solution. Characterization via Fourier Transform Infrared Spectroscopy (FT-IR) confirmed the presence of carbonaceous groups, such as C=O, C-O, C=C and derived phosphoric groups, such as P=O. Scanning Electron Microscopy-Energy Dispersive X-ray Spectroscopy (SEM-EDS) revealed a mesoporous and macroporous structure, while X-ray Diffraction (XRD) indicated a predominantly amorphous material containing amorphous SiO₂ phases. The adsorption was followed by monitoring 464 nm band of MO in UV-Vis spectroscopy, and the adsorbent achieved a maximum removal of above 89% of MO within a 60-minute experiment. The adsorption kinetics were analysed in pseudo-first and pseudo-second models, which the adsorption was described better by the pseudo-first-order model. Also, adsorption isotherms (Langmuir, Freundlich and Temkin) were studied, and the equilibrium data closely fit the Langmuir isotherm model, pointing to monolayer adsorption onto a homogeneous surface. The FT-IR analysis of post-adsorbed PS-BC confirmed bands associated with MO, such as N=N, SO₃ and change in aromatic C=C, indicating the possible adsorption pathways. These results confirm the successful application of the acid-treated PS-BC as an efficient and eco-friendly adsorbent for organic pollutant removal from water.

Keywords: Adsorption, Biochar, Contamination problems, Methyl Orange, Removal processy

1. INTRODUCTION

Nowadays, the environment is continuously impacted by the increasing release of pollutants into aqueous matrices, where, in many cases, these pollutants are not effectively removed by conventional water treatment processes. With growing environmental concerns, emerging contaminants have been a topic that has attracted the attention of several researchers and environmental protection regulations over the years [1–3].

Emerging contaminants (ECs) are pollutants derived from compounds commonly used in daily products, such as personal care products, plasticizers, pharmaceuticals, pesticides, surfactants, and others, which are hardly removed by conventional water treatment mechanisms [4, 5]. This occurs because ECs exhibit diverse chemical properties and are usually found in aqueous matrices at very low concentrations, which hinders their detection and removal measures [6].

In this context, aqueous contamination by synthetic dyes continues to increase due to their widespread demand in industries such as food, leather, polymers, cosmetics, electronics, and textiles [7, 8]. Currently, approximately 700.000 tons of synthetic organic dyes are produced worldwide each year, highlighting the relevance of this issue, as many of these dyes may be improperly discharged into aquatic matrices, thereby contributing to increased water pollution [9].

OPEN ACCESS

Affiliation

Institute of Physics and Chemistry, Federal University of Itajubá, 3500-903, Minas Gerais, Brazil.

*Correspondence

Email: ralf.junior@unifei.edu.br

ORCID

Erik S. Pereira: 0009-0002-4469-0034

Ralf R. R. Junior: 0000-0002-6638-193X

Sandro J. Andrade: 0000-0002-7520-840X

Received: March 28, 2026

Revised: April 27, 2026

Accepted: May 13, 2026

How to cite: Pereira, E.S., Junior, R.R.R., Andrade, S.J., (2026). Application of acidic treated peanut shell biochar in methyl orange removal from aqueous medium: Elucidating isotherms, kinetics and proposed mechanism. *Journal of Applied Materials and Technology*, 8(1), 1–9. <https://doi.org/10.31258/Jamt.8.1.1-9>.

Copyright (c) 2026 Erik S. Pereira, Ralf R. R. Junior, Sandro J. Andrade. This article is licensed under a [Creative Commons Attribution 4.0 International License](#).



Regarding Methyl Orange, it is widely used in the textile industry due to its characteristic color, which can be easily applied to various types of fabrics. In addition, it is commonly employed in laboratories as a pH indicator in titrations. Owing to its high solubility, it readily dissolves in water, making it a potential contaminant of aquatic environments even at low concentrations. In this context, different methods have been studied and applied for its removal from solutions, including advanced oxidation processes, photocatalytic degradation, ultrafiltration, electrochemical degradation, and coagulation-flocculation [10].

However, these methods present limitations, as they are often complex, require high operational costs, and involve time-consuming unit operations. In contrast, the adsorption technique stands out as a versatile alternative for contaminant removal, owing to its simplicity in design and operation, low sensitivity to the presence of toxic compounds, and reduced operational cost, as it can be carried out using readily available materials [10]. The application of low-cost materials in organic pollutants removal from aqueous medium has been an interesting trend in environmental sciences, such as agricultural waste, biomass as biosorbents. One example of agricultural waste is peanut shells, which are generated by processing the peanuts to food industry.

The production of peanut is about 539 million ton annually, which turns to produce a large number of agricultural wastes [11]. The selection of peanut shell waste as precursor is justified by its lignocellulosic composition, which provides a structural backbone for developing porosity and enhanced surface area. These inherent characteristics, combined with its abundance, enable its application as an efficient for the remediation of contaminants from aqueous medium [12]. The thermal treatment of the biomass produces biochar, a carbonaceous material that can enhance its application in contaminant removal and improves the recycling and the valorization of the peanut biomass generated waste [13–15].

Biochar is widely used for this purpose due to its excellent adsorptive properties. These properties arise from its structural characteristics, as it is a granular and porous solid material with a high specific surface area, a well-developed pore structure, and an abundance of surface functional groups. The combination of these attributes enhances the sorption process of contaminants in aqueous media, making it a highly effective resource for their removal [16].

Furthermore, due to its characteristics, biochar has gained prominence as a low-cost adsorbent, being extensively investigated by researchers worldwide, as a potential sustainable resource derived from agricultural waste. Its production occurs through the pyrolysis process, which, in the absence of oxygen, yields materials with high surface area and remarkable adsorption capacity [17–19]. Therefore, biochar stands out as an environmentally friendly technology for the removal of contaminants.

To improve the properties of biochar, it can be treated with chemical compounds to promote its activation, such as bases, acids, and metallic compounds [20]. Recent literature shows a trend toward developing engineered biochars through relatively complex synthetic routes. For instance, bamboo shoot shells biochar were synthesized by an initial in-situ pre-carbonization before acidic activation, adding extra thermal treatment and impacting in residence time [21]. Other synthetic route is hydrothermal carbonization, in the previous reported peanut shell hydrochar,

that required experimental control and had relatively high energy consumption [22]. Furthermore, recent trends in biochar research implies its modification, with metallic compounds for example, as reported by Sunthar et al., which demanded multi-step synthetic process [23].

Unlike the conventional synthesis of engineered biochar might require multiple thermic stages or expansive chemical functionalization, the use of phosphoric acid allows the obtaining of low-cost and simple activated biochar [20]. The use of phosphoric acid is justified by its several advantages, such as its effectiveness at moderate pyrolysis temperatures, its lower environmental impact, its ability to produce high-quality adsorbents, and its low cost [24, 25]. Also, studies have shown that phosphoric acid can act as an activating agent in carbon production, enhancing the porosity of carbonaceous structures in biochar, thereby improving their adsorption properties [26]. In addition, the application of this chemical activator increases the density of surface functional groups and enhances the surface roughness characteristics of treated biochar, highlighting the effectiveness and advantages of this process [27].

In this context, this present study aims to evaluate the application of peanut shell biochar (PS-BC), synthesized with phosphoric acid pre-treated peanut shell through a one-step pyrolysis treatment. This approach prioritizes a simplified synthetic route to obtain PS-BC, for the removal of the synthetic dye methyl orange from aqueous solutions. The obtained material was characterized, and the removal performance was assessed, along with kinetic and isotherm studies, under specific conditions designed to ensure effective dye removal.

2. EXPERIMENTAL

2.1. Material. In The peanut shells were collected from local market in Itajubá, Minas Gerais, Brazil. Phosphoric Acid was purchased from Sal-R (purity >85%). Sodium hydroxide (purity >97%) was purchased by Synth. Methyl Orange powder was purchased from Dinâmica (purity >98%).

2.2. Methods. 2.2.1. Synthesis of peanut shell biochar. Peanut shells collected from the local market in Itajubá, Minas Gerais, Brazil, were washed with distilled water. After dryage, the peanut shells were treated with H_3PO_4 (1.0 mol L^{-1}) for 60 minutes, followed by a dry process for 24 hours. The dry treated biomass was thermally treated in a sealed ceramic container, heating at a rate of $5 \text{ }^\circ\text{C min}^{-1}$ until it reached $600 \text{ }^\circ\text{C}$, a temperature which was set to 3h of thermal treatment. The resulting pH was treated with NaOH (1.0 mol L^{-1}) in an aqueous suspension to pH~7, to reduce the effects of PS-BC in altering pH values in removal experiments. The methodologic steps are represented in Figure 1.

2.2.2. Characterization. The prepared biochar was characterized by Fourier Transform Infrared Spectroscopy, FT-IR with attenuated total reflectance module (Spectrum 100, PerkinElmer®) from 650 cm^{-1} to 4000 cm^{-1} , with 16 scans; X-ray Diffraction, XRD (X'pert PRO, PANalytical®) from 10° to 80° of 2θ , $0.02^\circ \text{ s}^{-1}$ (with Cu X-ray source), and Scanning Electron Microscopy with Energy Dispersive Spectroscopy, SEM-EDS (EVO-MA 15, Zeiss®). The MO UV-Vis spectrum was analyzed using UV-Vis spectroscopy (K37, KASVI®) at 464 nm detection.

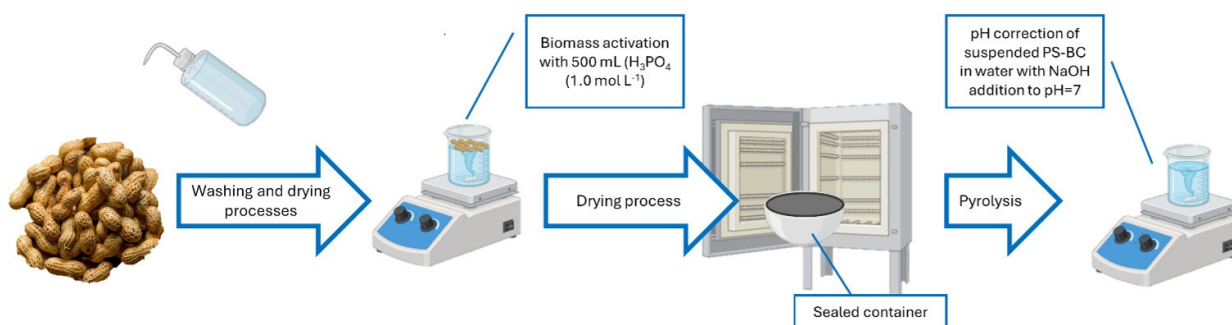


Figure 1. Synthesis of PS-BC by biomass activation with phosphoric acid.

2.2.3. Experiments for removal of methyl orange. The samples were analyzed in a UV-Vis spectrometer (K37, KASVI®), selecting the wavelength of 464 nm, corresponding to $\pi-\pi^*$ transition in the azolic group in the MO framework. A MO solution (10 mg L^{-1}) and PS-BC (1 g L^{-1}) were stirred for 60 minutes, in the removal experiments, which were made in triplicate. The sampling was performed at 5, 15, 30, 45 and 60 minutes. The dye removal was analyzed by UV-Vis spectroscopy (K37, KASVI®), selecting a wavelength of 464 nm, corresponding to the $\pi-\pi$ transition in the azo group.

The adsorption was also studied with kinetics, considering all sample points in the removal experiments, and analyzed using non-linear fitting. The Langmuir and Freundlich Isotherms were developed with 4 samples, at $20 \pm 1 \text{ }^\circ\text{C}$ and evaluated under linear adjustments, such as the Lineweaver-Burk for Langmuir isotherm and logarithm adjusted for Freundlich, as shown in Equations 1 and 2, respectively:

$$\frac{1}{q_e} = \frac{1}{q_{\max} K_L C_e} + \frac{1}{q_{\max}} \quad (1)$$

$$\log(q_e) = \log(K_F) + \frac{1}{n} \log(C_e) \quad (2)$$

Thus, it is possible to investigate the adsorption mechanism of MO in solution onto PS-BC and to determine which isotherm best describes this process. Furthermore, kinetic studies allow the evaluation of whether the removal follows a pseudo-first-order or pseudo-second-order model.

3. RESULT AND DISCUSSION

3.1. Material characterization. The characterization steps were applied to understand the material characteristics, such as FTIR, XRD, and SEM-EDS. In the FT-IR spectrum of the synthesized biochar, presented in Figure 2, characteristic cellulose-related stretching vibrations of the biomass can be observed, such as the C=O band around 1700 cm^{-1} and the C–O band near 1000 cm^{-1} . However, the pyrolysis process likely induced structural alterations in cellulose, as evidenced by the appearance of the C=C stretching band of aromatic rings at 1550 cm^{-1} , attributed to possible structural modifications. Furthermore, the P=O stretching band at 1200 cm^{-1} was also detected, confirming the activation of the biomass with phosphoric acid [21].

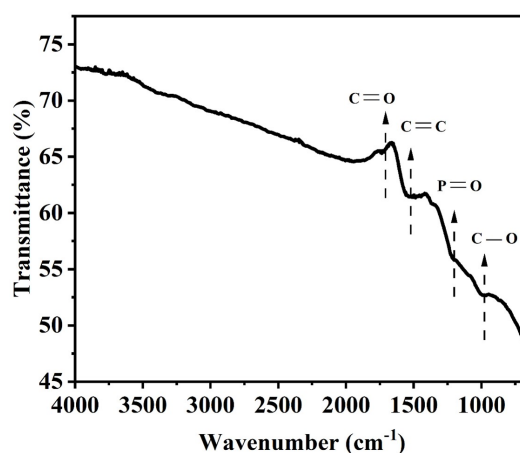


Figure 2. PS-BC spectrum by FT-IR.

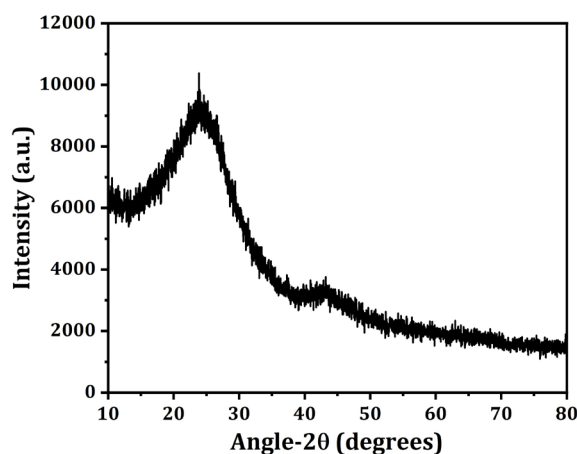


Figure 3. PS-BC PS-BC X-ray diffractogram 10-80° degrees scanning with broad response in 20-30°, associated with amorphous SiO_2

In the XRD diffractogram, shown in Figure 3, the material exhibits low crystallinity, evidenced by its response followed by a single broad signal at 2θ between 20° and 30° , which is typical of amorphous materials lacking a highly ordered molecular structure, but it can also to disordered aromatic carbon structures. This

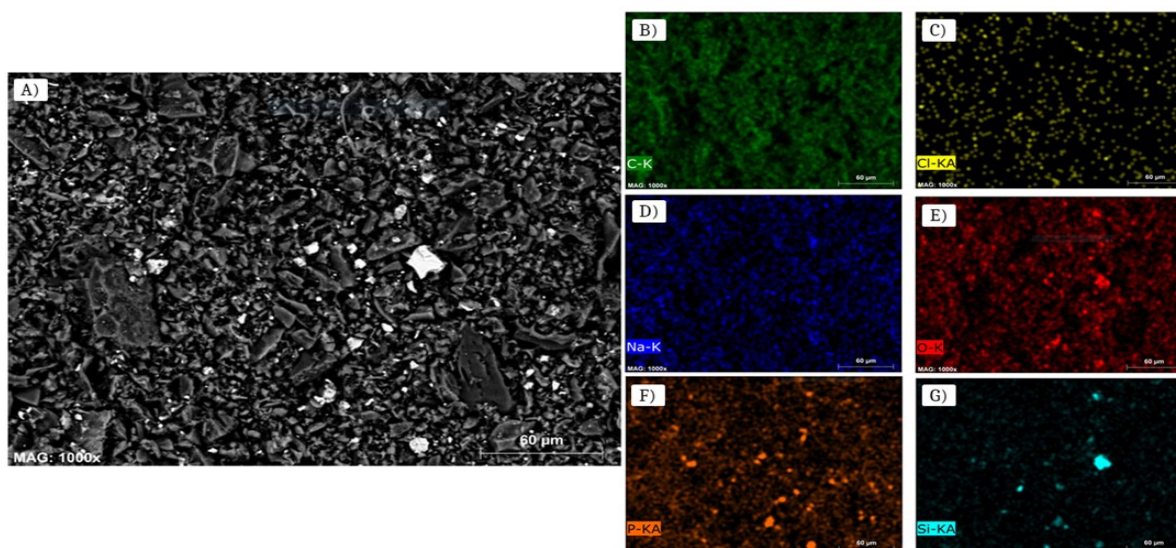


Figure 4. SEM image of PS-BC at 1000x magnification with general elemental mapping by EDS (A). Each subsequent image represents the distribution of a specific element: Carbon in green (B); Chlorine in yellow (C); Sodium in blue (D); Oxygen in red (E); Phosphorus in orange (F) and Silicon in cyan (G).

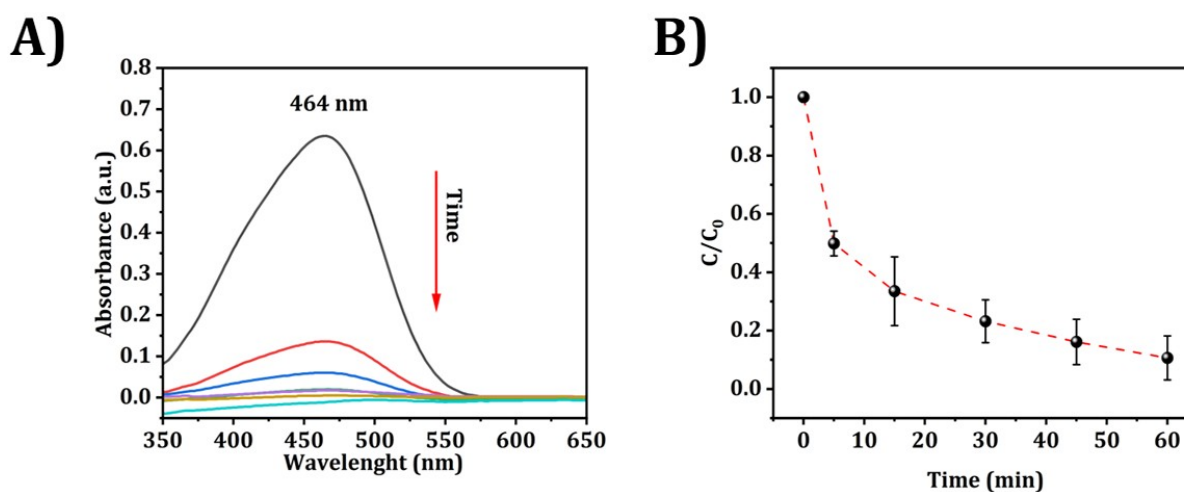


Figure 5. MO spectra through samples taken (A); C/C₀ result in the adsorption system (B).

alteration in the ligno-cellulosic structure may be associated with the pyrolysis process and the treatment with H₃PO₄, which both can promote depolymerization processes [28]. The XRD patterns approximates to the reported by Turk Sekulic et al. in developing PPhA biochar, also associating the signal in approximately 43° to the reflection plane of graphitic structures [26]. On the other hand, different types of biomasses might contain different mineral portions, such as the observed by Thabede & Shooto, associating the presence of KCl and CaCO₃ in the obtained biochars [29].

SEM-EDS micrographs, obtained by back scattering electrons, demonstrated scattered occurrences of macro porous structures, as shown in Figure 4A and in Figure S1, which can be associated with thermal treatment or certain characteristics of the biomass after the acidic activation. Figure S1 represents an SEM image of PS-BC at 1000x magnification with sections showing the pore profile about 10 μm² (A) and 4 μm² (B). The micrograph showed that the pores

exhibit a certain range of sizes, between 10 and 3.8 μm² pore area, according to a 1000x magnification micrograph. This fact can be attributed to the pyrolysis temperature, which can promote the formation of a larger number of pores lacking an organized crystalline arrangement [30]. Studies have reported that micropores exhibit internal diameters of up to 20 Å, while mesopores range between 20 and 500 Å [26]. In this context, PS-BC presented significantly larger pores, within the micrometer scale, thus being characterized as an agglomerate of macropores permeating its structure, as shown in Figure S1. Furthermore, it can be observed that the pores of PS-BC display distinct dimensions, a consequence of its low morphological organization, as corroborated by the X-ray diffraction analysis. Through the observed morphology, the biomass treatment with phosphoric acid can be associated to the meso and microporous structures, as seen in the work of Turk Sekulic et al. [26]. In comparison to the produced biochars from peanut shell,

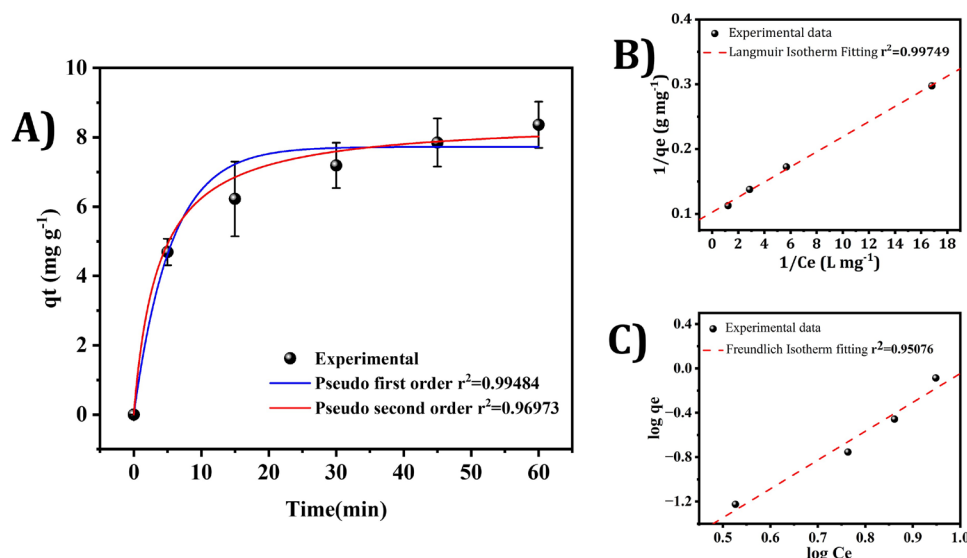


Figure 6. SEM Adsorption Kinetics (A); Langmuir isotherm fitting (B); Freundlich isotherm fitting (C).

PS-BC showed a morphology that approximates to peanut shell precursor structures with distributed pores, achieved with the acidic treatment of the biomass, while other peanut shell biochars demand more costive treatments, such as silicon modification, to enhance its porosity. Between other biomasses, PS-BC demonstrated relatively organized porosity, while another material, such as carrot and potato peels biochar previously reported in the literature, showed rougher structures [29].

Through the general EDS mapping, which semi-determinations response are represented in Figure 4B-G and Figure S2, it was possible to identify the presence of different elements in the biochar, including carbon and oxygen, from residues of cellulose, hemicellulose and lignin; phosphoric compounds from H_3PO_4 activation, which can be associated with phospho-organic compounds [26]; and sodium from pH adjustment.

The elements detected agreed with EDS mapping, pointing to the successful synthesis of acidic PS-BC. Small amounts of aluminum and silicon were detected, which may have originated from contaminants present in the peanut shell and subsequently retained after the pyrolysis process or originally from the biomass.

There are also reports in the literature indicating that the silicon detected through SEM-EDS analysis may be associated with the presence of amorphous SiO_2 on the biomass surface. Furthermore, another possible explanation is the formation of SiO_2 during the biochar pyrolysis process. This occurs due to the presence of silicon atoms on the agricultural waste surface, leading to the generation of this inorganic compound [31].

Moreover, it is important to emphasize that previous studies have shown that peanut shells, the precursor of the synthesized biochar, contain several inorganic elements in their matrix, such as sodium, potassium and aluminum [32]. This composition explains the results obtained from the EDS analysis; although present in significantly lower proportions compared to carbon and oxygen, these elements were still detectable in the composition of the synthesized PS-BC. Although biochar and biochar-based adsorbents materials with chemical activators have been widely used in previous studies,

PS-BC stands out for employing simplified activation process. This approach is relevant due the comparison with the complex and costly activation and biomass treatment, such as the treatment with multiple agents and the use of hydrothermal methods or utilizing extra carbonization steps and pretreatments [21, 33].

3.2. MO removal experiments. In the removal experiment, a linear approximation was considered by selecting the absorbance points at 465 nm. The following removal tests considered the adsorption experiments, which were performed at $\text{pH} = 6.8 \pm 0.1$ and showed a removal rate of $89.9 \pm 7.5\%$ of MO in a 60-minute experiment, which can be evidenced by the diminished UV-Vis spectra of MO throughout the time, as represented in Figure 5.

The kinetics and isotherms were studied and are presented in Figure 6. The adsorption kinetics study pointed to a better description of the pseudo-first order model, with correlation $r^2 = 0.99484$, compared to the pseudo-second order, with correlation $r^2 = 0.96973$, which can be attributed to the way in which removal occurs, as well as to the structural characteristics of the adsorbent and its interaction with the adsorbate [26]. The determination of separation factor (R_L) considered the following equation:

$$R_L = \frac{1}{1 + (K_L \times C_0)} \quad (3)$$

Where R_L is Langmuir's separation factor; K_L is Langmuir's constant; C_0 is the initial MO concentration. The resulting R_L was 0.011, and its analysis showed that adsorption is very favored (when R_L value gets near 0, in an interval between 0.00 - 1.00).

The Langmuir and the Freundlich isotherms fitting grant correlation of $r^2 = 0.99749$ and 0.95076, respectively, which can describe a monolayer adsorption process. Complementarily, Temkin isotherm was studied in Figure S3. The resulting q_{max} in the Langmuir model resulted in 9.77 mg g^{-1} maximum adsorptive performance, approaching previous report in literature [34]. The comparison between the non-linear adjustment showed a better description in the pseudo-first model, being associated with an adsorption process

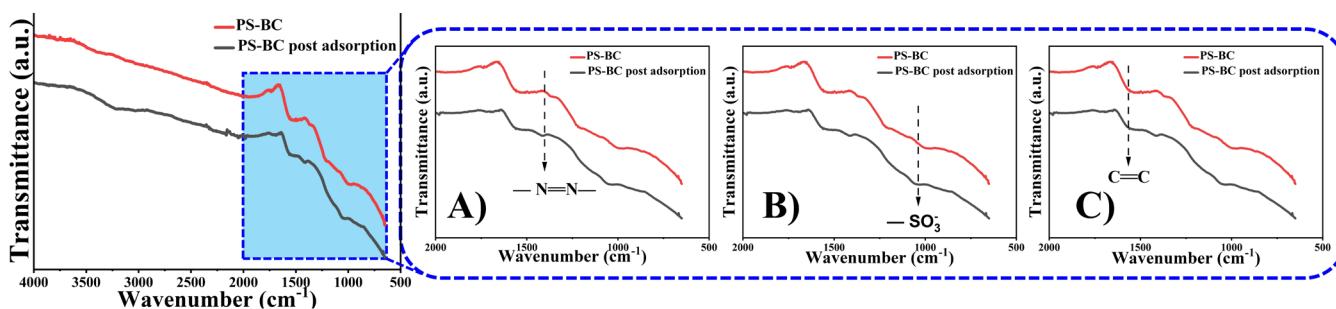


Figure 7. FTIR spectra before and after adsorption of MO: detected azolic (N=N) group stretching mode (1398 cm^{-1})(A); sulfonate stretching vibrational mode (1042 cm^{-1})(B); change in vibrational mode of aromatic C=C (1564 cm^{-1}) (C).

Table 1. Contaminants removal applying different biochar types.

Biochar type	Contaminant	Adsorbent dosage (g L^{-1})	Removal yield (%)	Kinetic model	Isotherm model	Reference
Sawdust	Methyl orange	1.0	~83.0	-	Langmuir	[34]
Engineered biochar from neem chips (with 7% FeCl_3)	Methyl orange	1.0	~80.3	PSO	Freundlinch	[23]
Phosphoric activated bamboo shoot shells	Methyl orange	1.0	~97.0	PSO	Langmuir	[21]
Peanut shell biochar	Naproxen	0.5	-	PSO	Langmuir	[22]
Carrot and potato peel	Methyl orange	1.0	~98.0	PSO	Langmuir	[29]
Coconut shell	Methyl blue	0.4	~95.0	PSO	Langmuir	[33]
Coconut coat	Methyl blue		~21.0	PSO	Langmuir	[33]
Wood residue treated with H_3PO_4	Sulfamethoxazole	1.0	~90.0	PSO	Langmuir	[26]
Corn Straw biochar	Sulfamethoxazole	1.0	~85.0	-	Freundlinch	[35]
H_3PO_4 treated Peanut Shell	Methyl orange	1.0	~89.0	PSO	Langmuir	This work

mediated not directly to chemisorption steps, but controlled by diffusion and mass transfer steps between MO and the PS-BC. The removal of other synthetic dyes is reported in literature, and can pose as comparison points in this work, as shown in Table 1.

The comparative works of MO seem to approximate the Langmuir isotherm model, pointing to monolayer adsorption process evolving the anionic dye, in agreement with the observed in this work. In kinetic terms, functionalized biochar, such as seen in the work of Sunthar et al., showed to follow PSO kinetic model, in comparison with pure biochars application, that followed PFO kinetic models. The type of biomass can influence the effects on adsorption kinetics, once the comparison between phosphoric acid treated biochars seem to lead to different kinetic models, even with the same contaminant (MO), in an analysis between the work of Xiang et al. and the results in this work [21]. Thus, it was observed that the sorption of MO proceeded in a manner that allowed for a detailed

analysis of the process. Regarding the sorption kinetics, the adsorption constant $k_1 = 0.1823$ was determined for the pseudo-first-order model, which provided the best fit for describing the removal of MO using PS-BC. The PS-BC was analyzed in FTIR before and after the adsorption process, to investigate the MO profile in BC after removal process, which is represented in Figure 7. In the FTIR spectra, the material after adsorption presented a band in 1398 cm^{-1} (Figure 7A), that can be related to azolic group (N=N) characteristic of MO organic framework, pointing to its presence on BC surface after removal process; the band in 1042 cm^{-1} (Figure 7B) can be associated to sulfonate group ($-\text{SO}_3^-$), which is associated to the anionic form of MO molecule; the changing in aromatic C=C bands in 1564 cm^{-1} between PS-BC and PS-BC post adsorption (Figure 7C) can be related to an indicative π - π interaction between the aromatic rings of MO and the ones in BC constitution. The adsorption proceeded in two observed steps: a fast adsorption (between 5 - 10

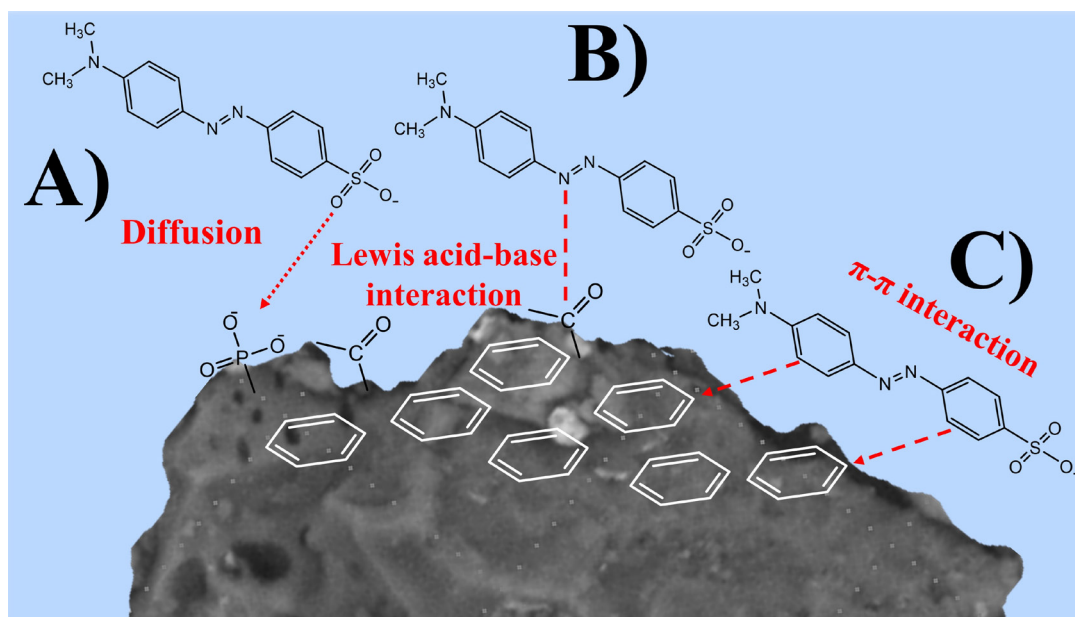


Figure 8. Proposed adsorption steps of MO onto PS-BC: Firstly, MO diffusion towards PS-BC (A); Lewis interaction with N from MO azo-group and C in carbonylic groups (B); Development of π - π interaction between aromatic groups of MO and PS-BC (C).

min), and a slow step of adsorption and equilibrium (between 30 - 60 min). In the beginning of the experiment, the pores of the PS-BC were fully available to the interaction with MO molecules, which has its sulfonated group in ionic form ($-\text{SO}_3^-$) and are attracted to the surface of PS-BC (Figure 7A); once N atoms has lone electron pairs, the azo-group ($\text{N}=\text{N}$) of MO perform Lewis acid-base interactions with carbonylic carbon atom or phosphorus atoms in phosphoric groups in PS-BC surface (Figure 7B); the aromatic moiety of MO molecules perform π - π interactions with aromatic structures in PS-BC (Figure 7C) [23, 34, 36]. The coordination of these three possible mechanisms can be associated to how favorable adsorption is ($R_L = 0.011$) and can be associated to the monolayer pattern in Langmuir model. Figure 8 represents a scheme of possible interactions between MO and PS-BC.

4. CONCLUSION

The contamination of water matrices with synthetic molecules causes an emerging interest in the application of materials for the removal of these contaminants. In this work, a synthesized PS-BC was characterized and demonstrated a promising yield in MO removal, with rates exceeding 80%. Kinetically, the adsorption process can be described by pseudo-first order, pointing to a mass transfer mediated process, which also follows the monolayer model adsorption, once the best isotherm fitting being the Langmuir model. The FTIR analysis after adsorption showed SO_3^- and $\text{N}=\text{N}$ groups attached to BC, and also interaction between aromatic rings of MO and BC.

Finally, based on this study, future investigations may focus on scaling up the synthesis process, more broadly evaluating the performance of PS-BC in real water samples, studying its potential for regeneration and reuse, to enhance its applicability, to explore its recyclability, and promote sustainable contaminants removal techniques.

ACKNOWLEDGEMENTS

The authors would like to thank the Federal University of Itajubá (UNIFEI), the Physics and Chemistry Institute (IFQ), the National Council for Scientific and Technological Development (CNPq), the Research Support Foundation of Minas Gerais (FAPEMIG) and the National Council for Improvement of Higher Education (CAPES). The research was supported by the National Council for Improvement of Higher Education (scholarship process number 88887.903838/2023-00) and by the National Council for Scientific and Technological Development (scholarship process number 139696/2025-3).

CREDIT AUTHOR STATEMENT

Pereira, E.S.: Formal analysis, Data curation, Investigation, Methodology, Validation, Writing-original draft. **Junior, R.R.R.:** Conceptualization, Data curation, Formal analysis, Investigation, Methodology, Supervision, Validation, Writing-original draft, Review and Editing conceptualized the study, developed the methodology, performed data curation. **Andrade, S.J.:** Funding acquisition, conceptualization, methodology, project administration, supervision, resources, writing-review and editing.

DECLARATIONS

Conflict of interest The authors declare that they have no known competing financial interests or personal relationships that could have appeared to influence the work reported in this paper.

■ AVAILABILITY OF DATA

The All data supporting the findings of this study are included within the manuscript. Any additional data related to this work is available from the corresponding author upon reasonable request.

■ AI DISCLOSURE STATEMENT

During the preparation of this work, the authors used Grammarly (v.1.2.236.1843) in order to improve the readability and language of the text. After using this tool, the authors reviewed and edited the content as needed and take full responsibility for the content of the publication.

■ REFERENCES

- [1] Morin-Crini N, Lichtfouse E, Liu G, Balaram V, Ribeiro ARL, Lu Z, et al. Worldwide cases of water pollution by emerging contaminants: a review. *Environ Chem Lett* 2022;20:2311–38. <https://doi.org/10.1007/s10311-022-01447-4>.
- [2] Li X, Shen X, Jiang W, Xi Y, Li S. Comprehensive review of emerging contaminants: Detection technologies, environmental impact, and management strategies. *Ecotoxicol Environ Saf* 2024;278. <https://doi.org/10.1016/j.ecoenv.2024.116420>.
- [3] Khan S, Naushad M, Govarthanam M, Iqbal J, Alfadul SM. Emerging contaminants of high concern for the environment: Current trends and future research. *Environ Res* 2022;207. <https://doi.org/10.1016/j.envres.2021.112609>.
- [4] Saidulu D, Gupta B, Gupta AK, Ghosal PS. A review on occurrences, eco-toxic effects, and remediation of emerging contaminants from wastewater: Special emphasis on biological treatment based hybrid systems. *J Environ Chem Eng* 2021;9:105282. <https://doi.org/10.1016/j.jece.2021.105282>.
- [5] Rivera-Utrilla J, Sánchez-Polo M, Ferro-García MÁ, Prados-Joya G, Ocampo-Pérez R. Pharmaceuticals as emerging contaminants and their removal from water. A review. *Chemosphere* 2013;93:1268–87. <https://doi.org/10.1016/j.chemosphere.2013.07.059>.
- [6] Taheran M, Naghdi M, Brar SK, Verma M, Surampalli RY. Emerging contaminants: Here today, there tomorrow! *Environ Nanotechnol Monit Manag* 2018;10:122–6. <https://doi.org/10.1016/j.enmm.2018.05.010>.
- [7] Natarajan S, Bajaj HC, Tayade RJ. Recent advances based on the synergetic effect of adsorption for removal of dyes from waste water using photocatalytic process. *J Environ Sci (China)* 2018;65:201–22. <https://doi.org/10.1016/j.jes.2017.03.011>.
- [8] Kordouli E, Bourikas K, Lycourghiotis A, Kordulis C. The mechanism of azo-dyes adsorption on the titanium dioxide surface and their photocatalytic degradation over samples with various anatase/rutile ratios. *Catal Today* 2015;252:128–35. <https://doi.org/10.1016/j.cattod.2014.09.010>.
- [9] Damahe D, Mayilswamy N, Kandasubramanian B. Biochar/metal nanoparticles-based composites for Dye remediation: A review. *Hybrid Advances* 2024;6:100254. <https://doi.org/10.1016/j.hybadv.2024.100254>.
- [10] Iwuzor KO, Ighalo JO, Emenike EC, Ogunfowora LA, Igwegbe CA. Adsorption of methyl orange: A review on adsorbent performance. *Current Research in Green and Sustainable Chemistry* 2021;4. <https://doi.org/10.1016/j.crgsc.2021.100179>.
- [11] Sawargaonkar G, Pasumarthi R, Kale S, Choudhari P, Rakesh S, Mutnuri S, et al. Valorization of peanut shells through biochar production using slow and fast pyrolysis and its detailed physicochemical characterization. *Frontiers in Sustainability* 2024;5. <https://doi.org/10.3389/frsus.2024.1417207>.
- [12] Aryee AA, Mpatani FM, Kani AN, Dovi E, Han R, Li Z, et al. A review on functionalized adsorbents based on peanut husk for the sequestration of pollutants in wastewater: Modification methods and adsorption study. *J Clean Prod* 2021;310:127502. <https://doi.org/10.1016/j.jclepro.2021.127502>.
- [13] Mian MM, Liu G. Recent progress in biochar-supported photocatalysts: Synthesis, role of biochar, and applications. *RSC Adv* 2018;8:14237–48. <https://doi.org/10.1039/c8ra02258e>.
- [14] Dai Y, Zhang N, Xing C, Cui Q, Sun Q. The adsorption, regeneration and engineering applications of biochar for removal organic pollutants: A review. *Chemosphere* 2019;223:12–27. <https://doi.org/10.1016/j.chemosphere.2019.01.161>.
- [15] Tan X, Liu Y, Zeng G, Wang X, Hu X, Gu Y, et al. Application of biochar for the removal of pollutants from aqueous solutions. *Chemosphere* 2015;125:70–85. <https://doi.org/10.1016/j.chemosphere.2014.12.058>.
- [16] Wang Y, Chen L, Zhu Y, Fang W, Tan Y, He Z, et al. Research status, trends, and mechanisms of biochar adsorption for wastewater treatment: a scientometric review. *Environ Sci Eur* 2024;36. <https://doi.org/10.1186/s12302-024-00859-z>.
- [17] Van Wesenbeeck S, Higashi C, Legarra M, Wang L, Antal MJ. Biomass Pyrolysis in Sealed Vessels. Fixed-Carbon Yields from Avicel Cellulose That Realize the Theoretical Limit. *Energy and Fuels* 2016;30:480–91. <https://doi.org/10.1021/acs.energyfuels.5b02628>.
- [18] Satpati GG, Devi A, Kundu D, Dikshit PK, Saravanabhupathy S, Rajlakshmi, et al. Synthesis, delineation and technological advancements of algae biochar for sustainable remediation of the emerging pollutants from wastewater—a review. *Environ Res* 2024;258. <https://doi.org/10.1016/j.envres.2024.119408>.
- [19] Chen Y, Xu F, Li H, Li Y, Liu Y, Chen Y, et al. Simple hydrothermal synthesis of magnetic MnFe₂O₄-sludge biochar composites for removal of aqueous Pb²⁺. *J Anal Appl Pyrolysis* 2021;156. <https://doi.org/10.1016/j.jaap.2021.105173>.
- [20] Ahmad A, Priyadarshini M, Yadav S, Ghangrekar MM, Surampalli RY. The potential of biochar-based catalysts in advanced treatment technologies for efficacious removal of persistent organic pollutants from wastewater: A review. *Chemical Engineering Research and Design* 2022;187:470–96. <https://doi.org/10.1016/j.cherd.2022.09.024>.
- [21] Xiang W, Gan L, Wang Y, Yang N, Wang W, Li L, et al. Enhanced adsorption performance of phosphoric acid activated biochar from in-situ pre-carbonized bamboo shoot shells. *Ind Crops Prod* 2025;226. <https://doi.org/10.1016/j.indcrop.2025.120719>.

- [22] Tomul F, Arslan Y, Kabak B, Trak D, Kendüzler E, Lima EC, et al. Peanut shells-derived biochars prepared from different carbonization processes: Comparison of characterization and mechanism of naproxen adsorption in water. *Science of the Total Environment* 2020;726. <https://doi.org/10.1016/j.scitotenv.2020.137828>.
- [23] Sunthar L, Asharp T, Nadarajah K. Insights into Mechanisms of Novel Engineered Biochar Derived from Neem Chips via Iron Catalyst for the Removal of Methyl Orange from Aqueous Phase. *Water Air Soil Pollut* 2023;234. <https://doi.org/10.1007/s11270-023-06187-x>.
- [24] Chu G, Zhao J, Huang Y, Zhou D, Liu Y, Wu M, et al. Phosphoric acid pretreatment enhances the specific surface areas of biochars by generation of micropores. *Environmental Pollution* 2018;240:1–9. <https://doi.org/10.1016/j.envpol.2018.04.003>.
- [25] Girgis BS, El-Hendawy A-NA. Porosity development in activated carbons obtained from date pits under chemical activation with phosphoric acid. n.d.
- [26] Turk Sekulic M, Boskovic N, Slavkovic A, Garunovic J, Kolakovic S, Pap S. Surface functionalised adsorbent for emerging pharmaceutical removal: Adsorption performance and mechanisms. *Process Safety and Environmental Protection* 2019;125:50–63. <https://doi.org/10.1016/j.psep.2019.03.007>.
- [27] Farhaneem N, Dimin MF, Shaaban A, Mohamad N. Optimization of Phosphoric Acid Treatment Biochar using Response Surface Method. *JAMT*; 2016.
- [28] Zhang J, Zhang B, Zhang J, Lin L, Liu S, Ouyang P. Effect of phosphoric acid pretreatment on enzymatic hydrolysis of microcrystalline cellulose. *Biotechnol Adv* 2010;28:613–9. <https://doi.org/10.1016/j.biotechadv.2010.05.010>.
- [29] Thabede PM, Shooto ND. The removal of methyl orange from water using biochar derived from a blend of carrot and potato peels. *Desalination Water Treat* 2025;324. <https://doi.org/10.1016/j.dwt.2025.101584>.
- [30] Ma X, Zhou B, Budai A, Jeng A, Hao X, Wei D, et al. Study of Biochar Properties by Scanning Electron Microscope–Energy Dispersive X-Ray Spectroscopy (SEM-EDX). *Commun Soil Sci Plant Anal* 2016;47:593–601. <https://doi.org/10.1080/0103624.2016.1146742>.
- [31] Diagboya PN, Mtunzi FM, During RA, Olu-Owolabi BI. Empirical assessment and reusability of an eco-friendly amine- functionalized SBA-15 adsorbent for aqueous ivermectin. *Ind Eng Chem Res* 2021;60:2365–73. <https://doi.org/10.1021/acs.iecr.0c05115>.
- [32] Kwikima MM, Mateso S, Chebude Y. Potentials of agricultural wastes as the ultimate alternative adsorbent for cadmium removal from wastewater. A review. *Sci Afr* 2021;13. <https://doi.org/10.1016/j.sciaf.2021.e00934>.
- [33] Xu J, Fu M, Ma Q, Zhang X, You C, Shi Z, et al. Modification of biochar by phosphoric acid via wet pyrolysis and using it for adsorption of methylene blue. *RSC Adv* 2023;13:15327–33. <https://doi.org/10.1039/d3ra00680h>.
- [34] Abdulrahman Hanoon M, Ahmed MJ. Adsorption of Methyl Orange from Wastewater by using Biochar. *Iraqi Journal of Chemical and Petroleum Engineering* 2019;20:23–9. <https://doi.org/10.31699/ijcpe.2019.3.4>.
- [35] Zheng H, Wang Z, Zhao J, Herbert S, Xing B. Sorption of antibiotic sulfamethoxazole varies with biochars produced at different temperatures. *Environmental Pollution* 2013;181:60–7. <https://doi.org/10.1016/j.envpol.2013.05.056>.
- [36] Kataya G, Issa M, Badran A, Cornu D, Bechelany M, Jellali S, et al. Dynamic removal of methylene blue and methyl orange from water using biochar derived from kitchen waste. *Sci Rep* 2025;15. <https://doi.org/10.1038/s41598-025-14133-6>.